ORIGINAL ARTICLE

Sand blows as a potential tool for magnitude estimation of pre-instrumental earthquakes

Raymi A. Castilla · Franck A. Audemard

Abstract A worldwide database of liquefaction-induced sand blows has been compiled to generate empirical relationships between earthquake parameters and sand blow geometries. Curves resulting from these empirical relationships can be used afterwards for the study of historic and pre-historic earthquakes that formed sand blows. This database only incorporates instrumental earthquakes inducing sand blows, characterised in terms of magnitude (Mw), hypocentral location and focal mechanism solution. Two relationships are herein presented. The first curve, minimum likelihood of liquefaction occurrence (magnitude/epicentral distance), displays a logarithmic behaviour, as others already proposed. The second curve of sand-blow diameter vs epicentral distance is the first proposal of this kind, whose shape follows a negative power-law. Magnitude estimations of (pre-)historic earthquakes then may be attempted through these empirical relationships. Resulting magnitudes derived from these curves should be mostly considered as underestimated. The curves will reflect actual magnitudes only if, correspondingly, the farthest and largest blow has ever been reported during the after-earthquake survey. Following the same principle, a magnitude estimation resulting from the measuring of a sand blow can only be considered as minimal because it is almost impossible to ascertain that the measured feature is the biggest one produced by the earthquake under evaluation. Finally, these results call for thorough surveys of induced effects after every future moderate-to-large earthquake, as any empirical relationship simply improves by incorporating new data.

Keywords Earthquake magnitude · Epicentral distance · Sand blows · Historical seismology · Paleo-seismology

R. A. Castilla · F. A. Audemard (✉)
Earth Sciences Department, Venezuelan Foundation for Seismological Research (FUNVISIS),
Apdo. Postal 76880, Caracas 1070-A, Venezuela
e-mail: faudemard@funvisis.gob.ve

F. A. Audemard
Geology Department, School of Geology, Geophysics & Mines, Universidad Central de Venezuela,
Caracas, Venezuela

1 Introduction

Sediment liquefaction is the transformation of saturated granular material from a solid state into a fluid mass as a consequence of increased pore-water pressure during strong shaking (i.e. Munson and Munson 1996). It is a complex process resulting

from the combination of several and diverse favouring factors, both external (earthquake magnitude, duration of shaking, general site conditions) and internal to the liquefaction-prone sediment (confinement, pore pressure, grain size, packing, sorting and fine content, among several others). This process leads to the formation of sedimentary structures that can be preserved in the geological record as witnesses of past ground shaking. Among these are sand dykes or venting fractures, sand blows or boils, sand-filled burrows and lateral spreading, together with load casts, ball and pillows, flames and dish and pillars, among several others, which are extensively described in the literature (e.g. Audemard and De Santis 1991; Maltman 1994; Obermeier 1996; Alfaro et al. 1997). Obermeier (1996) states that distinctive earthquake-induced liquefaction features are only sand dykes, sand blows and lateral spreads because some of the other structures can also be formed in response to loading, compaction and/or water seepage. The growing use of the entire range of liquefaction features for the recognition of earthquakes (e.g. Sims 1973, 1975; Davenport and Ringrose 1987; Audemard and De Santis 1991; Tuttle and Seeber 1991; Obermeier 1996; Beck et al. 1996; Mörner 1996; Munson and Munson 1996; Alfaro et al. 1997; Tröften and Mörner 1997; Sukhija et al. 1999; Rodríguez Pascua et al. 2000; Mörner 2003; among many others) has been limited by the complexity and diversity of such structures (inherent to its genesis) and their not-so-clear relationship with the causative earthquake characteristics. In most cases, this geologic evidence of seismic shaking is used in a qualitative way, although several attempts have been made to establish clearer links between some source parameters and the liquefaction features (Kuribayashi and Tatsuoka 1975; Youd and Perkins 1987; Ambraseys 1991; Barlett and Youd 1992; Papadopoulos and Lefkopoulos 1993; Munson et al. 1995; Galli 2000; Castilla and Audemard 2002; Rodríguez et al. 2002; Rodríguez Pascua et al. 2003; Papathanassiou et al. 2005; Rodríguez et al. 2006).

This paper presents numerical relationships between isolated sand blows (Fig. 1) and the source characteristics of the related seismic event, thereby providing a way to infer the location and size of a past earthquake on the basis of the liquefaction features produced by it.

2 Methodology

To fulfil the fore-mentioned aim, a database of 67 sand blow descriptions related to 30 earthquakes was compiled from the literature and from our own Venezuelan Foundation for Seismological Research experience (Table 1). The gathered information is only related to recent earthquakes, characterised by available instrumental parameters. When possible, the epicentral location, focus depth and magnitude (Mw) were extracted from the Harvard Centroid-Moment-Tensor catalogue and USGS National Earthquake Information Center database to standardise this information. Local data were included when the seismic event was not available in the above-mentioned databases.

Regarding the sand boils, only those with location and shape parameters were included in the database. Special attention was given to sand boils for two reasons: (1) they correspond with the most reported liquefaction feature in the reviewed documents and (2) together with sand dykes, they are the most reliable sedimentary structures for identifying earthquakes in the geological record. As previously mentioned, they are unequivocal evidence of upward-directed hydraulic force suddenly applied to cohesionless sediments (Obermeier 1996). In addition, when sand blows form solely in response to hydraulic fracturing, the volume of expelled sediment and, therefore, their size is largely controlled by the earthquake magnitude (Atkinson et al. 1984) This relationship is less straightforward for blows associated with lateral spreading and those that use pre-existing conduits such as burrows, rotten roots, open cracks or fractures. When possible, the mechanism of cap failure was considered, identifying processes of lateral spreading or ground oscillation that could have enhanced the development of dykes and sand boils.

Some earthquake parameters, such as local intensity, acceleration and duration of the ground motion, could not be taken into consideration because they were unavailable.

3 Empirical relationships

Two cross-plots result from the database collected (Table 1): Earthquake magnitude vs distance between epicentre and induced sand boils (hereafter simplified
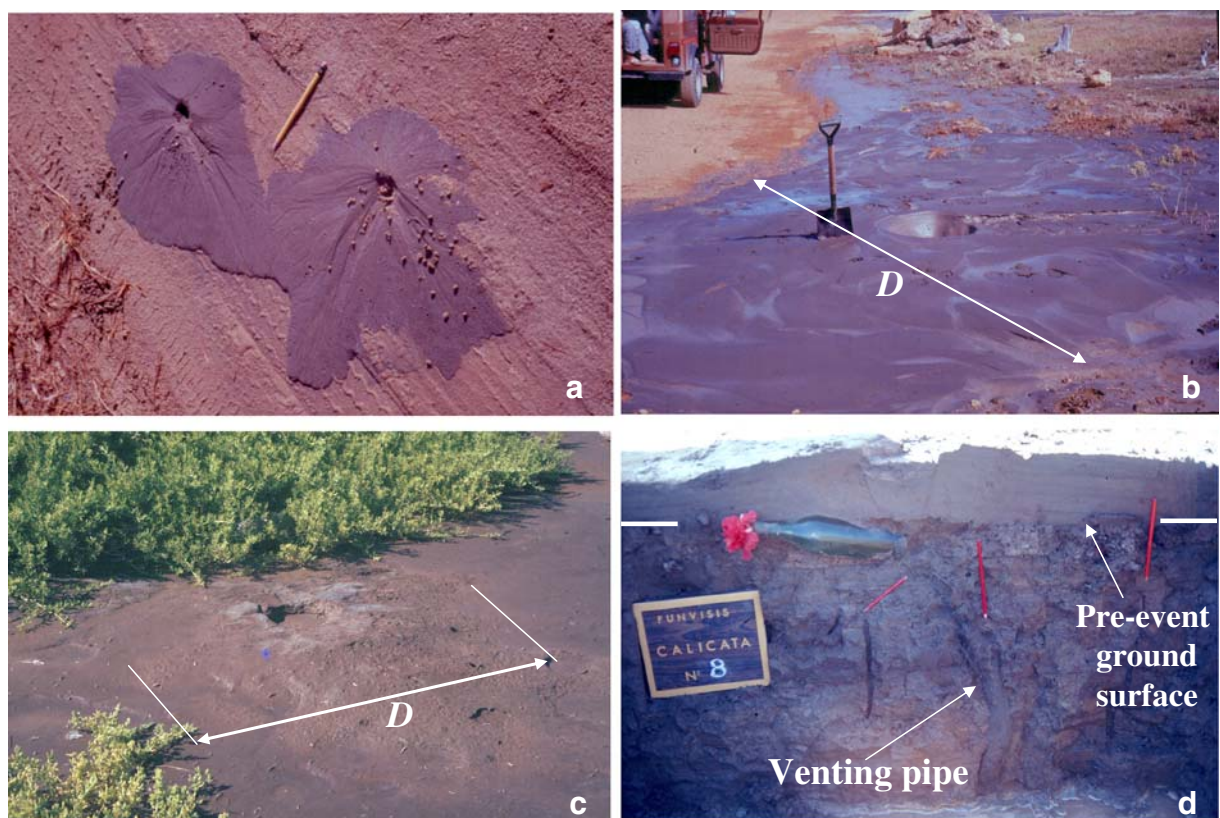
Fig. 1 Examples of isolated sand boils formed in association with the Boca de Tocuyo 1989 Mw 5.9 earthquake. **a**, **b** Freshly vented greyish sand boils, in the days following the main event (courtesy of Carlos Beltrán, an ex-colleague at the Venezuelan Foundation for Seismological Research). These two sand blows are given as end member examples of the wide range in size displayed by these features. **c** Aspect of a sand blow after 8 months of sub-aerial exposure (photo taken in December 1989), which is about 1.2 m across (*D*). Oxidation turned its original grey colour to brown, which makes its recognition very difficult. **d** Small (1×1×0.75 m deep) pit, exposing the sub-surface under the boil shown in **c**. The cone mouth and profile are easily distinguishable above the pre-event ground level, as well as the very fine lamination in the cone fine-grained sands. Also note the feeding conduit connected to the sand boil cone mouth (line drawing of this pit no. 8 is provided in Fig. 6 of Audemard and De Santis 1991)

as epicentral distance), and sand boil diameter vs epicentral distance, which are presented next.

3.1 Magnitude vs epicentral distance relationship

The magnitude vs epicentral distance of sand boils has been plotted with different symbols according to the type of focal mechanism solution (strike-slip, normal or thrust) for each single earthquake (Fig. 2). It can be seen that the collected earthquake population, regardless of the faulting type, shows a wide magnitude distribution (4.6<Mw<9.2). However, the larger events are mainly of the thrust type (essentially ≥Mw 7.0). Besides, most of the liquefaction data are located between magnitudes 5.5 and 7.5 and within the interval 0–150 km of epicentral distance, with very few exceptions. A boundary curve can be drawn along the lower limit of the data set points (with only one exception), dividing the graph into two fields. Below it, liquefaction susceptibility should be very low.

This lower-bound curve shows a logarithmic increase of the magnitude Mw with increasing epicentral distance Re. The equation that defines such curve is as follows:

$$Mw = 2.44 \text{Log}(Re) + 1.95 \qquad (1)$$

The curve described by Eq. 1 (Fig. 2), which bounds the worldwide data set herein collected, is constrained by the reverse and strike-slip-related data

Table 1 Collected database on worldwide earthquakes exhibiting liquefaction occurrence and related structures

SB_ID	Earthquake common name/ country	Earthquake information					Liquefaction locality	Liquefaction information				Reference
		Date	Earthquake location		Magnitude (Mw)	Focal solution		Liquefaction site location		Epicentral distance (km)	Sand blow diameter (cm)	
			Longitude	Latitude				Longitude	Latitude			
1	Anchorage/USA	27/ 03/ 1964	−147.73	61.04	9.2	Reverse	South bank of Portage Creek	−148.99	60.82	72.2	75	Walsh and Black 1995
2	Anchorage/USA	27/ 03/ 1964	−147.73	61.04	9.2	Reverse	South bank of Portage Creek	−148.98	60.82	71.9	20	Walsh and Black 1995
3	Niigata/Japan	16/ 06/ 1964	139.10	38.30	7.5	Reverse	Niigata, Japan	–	–	56	–	Seed and Idriss 1967
4	Guatemala	04/ 02/ 1976	−89.10	15.30	7.5	Strike-slip	Lake Amatitlan, near Guatemala city.	–	–	177	–	Page 1976
5	Bucharest/ Romania	04/ 03/ 1977	26.76	45.77	7.5	Reverse	Zimnicea, Romania.	–	–	260	50	Ambraseys and Despeyroux 1978
6	San Juan/ Argentina	23/ 11/ 1977	−67.77	−31.03	7.4	Reverse	San Juan Province, Argentina.	–	–	70	50	INPRES 1977
7	Miyagi-Oki/Japan	12/ 06/ 1978	142.07	38.02	7.6	Reverse	Miyagi Prefecture, Japan	–	–	110	–	Yamamura et al. 1979
8	Miyagi-Oki/Japan	12/ 06/ 1978	142.03	38.19	7.6	Reverse	Old Katami River, Japan.	–	–	103	100	Ellingwood 1980
9	El-Asnam/Algeria	10/ 10/ 1980	1.61	36.20	7.1	Reverse	Algeria	–	–	20	200	Leeds 1983
10	Eureka/USA	08/ 11/ 1980	−124.36	41.14	7.3	Strike-slip	Klamath river delta, CA	–	–	43.7	2500	Field et al. 1982
11	Nihonkai-Chubu/ Japan	26/ 05/ 1983	138.87	40.44	7.7	Reverse	Wakami, Japan	–	–	150	–	Yasuda and Tohno 1988

No.	Site	Date	Lon	Lat	Mag	Type	Location					Reference
12	Borah Peak/USA	18/10/1983	−113.86	44.06	7.0	Normal	Pahsimeroi Valley, USA	—	—	66	—	Waag and Lane 1985
13	Borah Peak/USA	18/10/1983	−113.86	44.06	7.0	Normal	Big Lost River valley, USA	—	—	12.4	1600	Waag and Lane 1985
14	Borah Peak/USA	18/10/1983	−113.86	44.06	7.0	Normal	Big Lost River valley, USA	—	—	9.3	500	Waag and Lane 1985
15	Borah Peak/USA	18/10/1983	−113.86	44.06	7.0	Normal	Big Lost River valley, USA	—	—	12.4	630	Waag and Lane 1985
16	Borah Peak/USA	18/10/1983	−113.86	44.06	7.0	Normal	Big Lost River valley, USA	—	—	12.4	2600	Waag and Lane 1985
17	Chile	03/03/1985	−71.98	−33.16	7.9	Reverse	San Antonio Harbor, Chile	−71.61	−33.61	60.7	—	Wyllie 1986
18	Edgecumbe/New Zealand	14/03/1987	176.80	−37.90	6.5	Normal	Whakatane, New Zealand	177.04	38.01	24.5	—	Pender and Robertson 1987
19	Edgecumbe/New Zealand	14/03/1987	176.80	−37.90	6.5	Normal	Around Edgecumbe, New Zealand	—	—	16.5	—	Pender and Robertson 1987
20	Greece	16/10/1988	20.9	37.95	5.9	Strike-slip	NW Peleponnesus, Greece.	—	—	15	130	Mariolakos et al. 1989
21	Saguenay/Canada	25/11/1988	−71.18	48.12	5.8	Strike-slip	Bras Hamel, Quebec, Canada.	—	—	26	1000	Tuttle et al. 1992
22	Saguenay/Canada	25/11/1988	−71.18	48.12	5.8	Strike-slip	Riviere des Ha! Ha!, Canada.	—	—	30	750	Tuttle et al. 1992
23	Saguenay/Canada	25/11/1988	−71.18	48.12	5.8	Strike-slip	Bras Hamel, Quebec, Canada.	—	—	26	100	Tuttle et al. 1992
24	Saguenay/Canada	25/11/1988	−71.18	48.12	5.8	Strike-slip	Ferland, Canada.	—	—	26.3	100	Tuttle et al. 1990
25	Saguenay/Canada	25/11/1988	−71.18	48.12	5.8	Strike-slip	Riviere Pikauba, Canada.	—	—	11	1500	Tuttle et al. 1992

Table 1 (continued)

SB_ID	Earthquake common name/country	Earthquake information					Liquefaction locality	Liquefaction information			Sand blow diameter (cm)	Reference
		Date	Earthquake location		Magnitude (Mw)	Focal solution		Liquefaction site location		Epicentral distance (km)		
			Longitude	Latitude				Longitude	Latitude			
26	Saguenay/Canada	25/11/1988	−71.18	48.12	5.8	Strike-slip	Ferland, Canada.	–	–	25.6	100	Tuttle et al. 1990
27	Saguenay/Canada	25/11/1988	−71.18	48.12	5.8	Strike-slip	Ferland, Canada.	–	–	25.6	1000	Tuttle et al. 1990
28	Saguenay/Canada	25/11/1988	−71.18	48.12	5.8	Strike-slip	Ferland, Canada.	–	–	25.6	10	Tuttle et al. 1990
29	Saguenay/Canada	25/11/1988	−71.18	48.12	5.8	Strike-slip	Ferland, Canada.	–	–	26.3	300	Tuttle et al. 1990
30	Saguenay/Canada	25/11/1988	−71.18	48.12	5.8	Strike-slip	Ferland, Canada.	–	–	25.6	10	Tuttle et al. 1990
31	Saguenay/Canada	25/11/1988	−71.18	48.12	5.8	Strike-slip	Riviere des Ha! Ha!, Canada.	–	–	30	750	Tuttle et al. 1992
32	Saguenay/Canada	25/11/1988	−71.18	48.12	5.8	Strike-slip	Ferland, Quebec, Canada.	–	–	25.6	75	Tuttle et al. 1990
33	Armenia	07/12/1988	44.36	41.10	7.0	Reverse	Pambak Valley, Armenia	–	–	15.5	–	Wyllie and Filson 1989
34	Boca del Tocuyo/Venezuela	30/04/1989	−68.18	11.10	5.9	Strike Slip > Normal	Boca del Tocuyo, Venezuela	−68.34	11.04	18.6	220	Audemard and De Santis 1991
35	Boca del Tocuyo/Venezuela	30/04/1989	−68.18	11.10	5.9	Strike Slip > Normal	Boca del Tocuyo, Venezuela	−68.34	11.04	18.6	700	Audemard and De Santis 1991
36	Boca del Tocuyo/Venezuela	04/05/1989	−68.21	11.14	5.5	Strike Slip > Normal	Boca del Tocuyo, Venezuela	−68.34	11.04	17.5	220	Audemard and De Santis 1991

No	Earthquake/Country	Date	Long	Lat	Mw	Fault type	Site	Long	Lat			Reference
37	Boca del Tocuyo/Venezuela	04/05/1989	−68.21	11.14	5.5	Strike Slip > Normal	Boca del Tocuyo, Venezuela	−68.34	11.04	17.5	244	Audemard and De Santis 1991
38	Boca del Tocuyo/Venezuela	04/05/1989	−68.21	11.14	5.5	Strike Slip > Normal	Boca del Tocuyo, Venezuela	−68.34	11.04	17.5	244	Audemard and De Santis 1991
39	Boca del Tocuyo/Venezuela	04/05/1989	−68.21	11.14	5.5	Strike Slip > Normal	Chichiriviche, Venezuela	−68.28	10.91	26.4	–	Audemard and De Santis 1991
40	Boca del Tocuyo/Venezuela	04/05/1989	−68.21	11.14	5.5	Strike Slip > Normal	Boca del Tocuyo, Venezuela	−68.34	11.04	17.5	220	Audemard and De Santis 1991
41	Boca del Tocuyo/Venezuela	04/05/1989	−68.21	11.14	5.5	Strike Slip > Normal	Boca del Tocuyo, Venezuela	−68.34	11.04	17.5	–	Audemard and De Santis 1991
42	Boca del Tocuyo/Venezuela	04/05/1989	−68.21	11.14	5.5	Strike Slip > Normal	Tocuyo de la Costa, Venezuela	−68.41	11.03	24.3	–	Audemard and De Santis 1991
43	Boca del Tocuyo/Venezuela	04/05/1989	−68.21	11.14	5.5	Strike Slip > Normal	Boca de Mangle, Venezuela	−68.4	11.14	20.2	5	Audemard and De Santis 1991
44	Loma Prieta/USA	17/10/1989	−121.88	37.04	6.9	Reverse > Strike-slip	Soda Lake, San Francisco, USA	–	–	30	500	Sims and Garvin 1995
45	Manjil/Iran	20/06/1990	49.40	37.00	7.4	Strike-slip	Loshan, Iran	–	–	22	76	Yegian et al. 1995
46	Luzon/Philippine	16/07/1990	121.23	15.97	7.7	Strike-slip	Dagupan city, Philippines	–	–	100	–	Kojima et al. 1992
47	Loma Prieta (aftershock)/USA	23/03/1991	−121.74	36.96	4.6	Reverse (Strike-slip	Soda Lake, San Francisco, USA	–	–	13	500	Sims and Garvin 1995
48	Loma Prieta (aftershock)/USA	23/03/1991	−121.68	36.92	5.5	Reverse > Strike-slip	Soda Lake, San Francisco, USA	–	–	2	500	Sims and Garvin 1995
49	El Limón/Costa Rica	22/04/1991	−83.07	9.69	7.6	Reverse	Limón, Costa Rica	–	–	40	200	López et al. 1992
50	El Limón/Costa Rica	22/04	−82.77	10.10	7.6	Reverse	Ports of Limon and Moin, Costa Rica	–	–	48	–	Singh et al. 1991

Table 1 (continued)

SB_ID	Earthquake common name/country	Earthquake information					Liquefaction locality	Liquefaction information				Reference
		Date	Earthquake location Longitude	Latitude	Magnitude (Mw)	Focal solution		Liquefaction site location Longitude	Latitude	Epicentral distance (km)	Sand blow diameter (cm)	
51	Roermond/The Netherlands	13/ 04/ 1992	5.80	51.15	5.4	Normal	Roer river, The Netherlands	–	–	10	240	Davenport et al. 1994
52	Petrolia/Canada	25/ 04/ 1992	−124.31	40.25	7.2	Reverse	CA, USA	–	–	4	30	Prentice et al., 1992
53	Egio/Greece	15/ 06/ 1995	22.46	38.10	6.5	Normal	Dead sea	–	–	5	50	Lekkas et al. 1996
54	Izmit/Turkey	17/ 08/ 1999	29.97	41.01	7.6	Strike-slip	Hastane (Adapazari), Turkey	–	–	42	–	Bakir et al. 2002
55	Chi-Chi/Taiwan	21/ 09/ 1999	120.98	23.77	7.6	Reverse	Yuan-Lin, Taiwan	120.69	23.77	29.5	100	NSF 2001 (Webpage currently unavailable)
56	Bhuj (Gujarat)/ India	26/ 01/ 2001	70.23	23.42	7.7	Reverse	Near Umedpur, India	–	–	45	32000	Tuttle 2001
57	Bhuj (Gujarat)/ India	26/ 01/ 2001	70.23	23.42	7.7	Reverse	Village south of Manfara, India	70.35	23.48	14	–	Tuttle 2001
58	Bhuj (Gujarat)/ India	26/ 01/ 2001	70.23	23.42	7.7	Reverse	North of Budharmora, India	70.19	23.34	9.3	50	Tuttle 2001
59	Bhuj (Gujarat)/ India	26/ 01/ 2001	70.23	23.42	7.7	Reverse	Allah Bund, India	–	–	130	200	Tuttle 2001
60	Bhuj (Gujarat)/ India	26/ 01/ 2001	70.23	23.42	7.7	Reverse	30 km north of Allah Bund, India	–	–	120	200	Tuttle 2001
61	Bhuj (Gujarat)/ India	26/ 01/ 2001	70.23	23.42	7.7	Reverse	Allah Bund, India	–	–	100	80	Tuttle 2001

62	Bhuj (Gujarat)/ India	26/ 01/ 2001	70.23	23.42	7.7	Reverse	Rann northwest of Chobari, India	—	15	1000	Tuttle 2001
63	Bhuj (Gujarat)/ India	26/ 01/ 2001	70.23	23.42	7.7	Reverse	Mud flats near Kandla Port, India	—	50	700	Tuttle 2001
64	Arequipa/Peru	23/ 06/ 2001	−72.71	−17.28	8.4	Reverse	Camaná river, Peru	—	150	200	Audemard et al. 2002
65	Arequipa/Peru	23/ 06/ 2001	−72.71	−17.28	8.4	Reverse	Between La Curva and El Arenal, Peru	—	340	100	Audemard et al. 2002
66	Arequipa/Peru	23/ 06/ 2001	−72.71	−17.28	8.4	Reverse	Yauca river, Peru	—	270	140	Audemard et al. 2002
67	Arequipa/Peru	23/ 06/ 2001	−72.71	−17.28	8.4	Reverse	Los Baños Bridge, Sama river, Peru	—	435	50	Audemard et al. 2002

(*Harvard Centroid-Moment-Tensor Catalog; **USGS)

set in the short- and mid-range distances (<250 km), whereas it is bounded only by one thrust-related liquefaction event for the wide and very wide distributions (250 up to 450 km). This fact can be biased by the distribution of the size of the largest earthquake by type of faulting. Figure 3 shows the clear zoning of event magnitudes by focal mechanism solution types, as expected. This figure also shows an unconventional distribution for strike-slip and thrust faulting ruptures, which could be imputed to lacking information around magnitude 6.5.

The following can also be derived from Fig. 2: (1) Sand boils associated to normal faulting take place mainly in the local field (Re<30 km), even for large earthquakes. (2) Similar distribution to the former is shown by sand boils induced by strike-slip mechanism, but extending up to a Re of 50 km. This may be biased by the collected set of earthquakes, as depicted in Fig. 3. (3) Sand boils induced by thrust faulting have a much wider spatial distribution than those of other types of faulting, particularly for events above Mw 7.2–7.3. (4) Liquefaction events associated to strike-slip faulting occur at a larger epicentral distance (Re) for earthquake magnitudes in the range below Mw 7.3 than for earthquakes with other types of faulting.

Figure 4 depicts two other lower-bound curves for comparison. These other curves not only use sand boils as ours (Fig. 2), but they are based on data sets of all types of earthquake-triggered liquefaction features with particular and different regional coverage, as several relationships already published. For instance, Galli (2000) proposes several bounding curves for the Italian catalogue. However, Galli's Eq. 14, correlating Me (equivalent magnitude; similar to Mw, after Galli's personal communication, 2007) vs epicentral distance for earthquakes in the period 1117–1990, is particularly very similar to the bounding curve proposed in this work (Eq. 1; Figs. 2 and 4). This similarity is almost perfect for magnitudes up to 7. For illustration and comparison purposes, we have reported in Fig. 4 only classes A4 (sand boils) and A5 (mud volcanoes) from Galli's catalogue, which are supportive of both his own curve and ours. This figure also depicts the curve proposed by Papathanassiou et al. (2005) for the Aegean region, as well as the sand boils reported by these authors. This last curve shows events with a larger extent of liquefaction occurrence above Ms 6.0. Besides, it appears that both data sets – of Galli

Fig. 2 Cross plot of earthquake magnitude vs epicentre-to-liquefaction feature distance, based only on sand blows
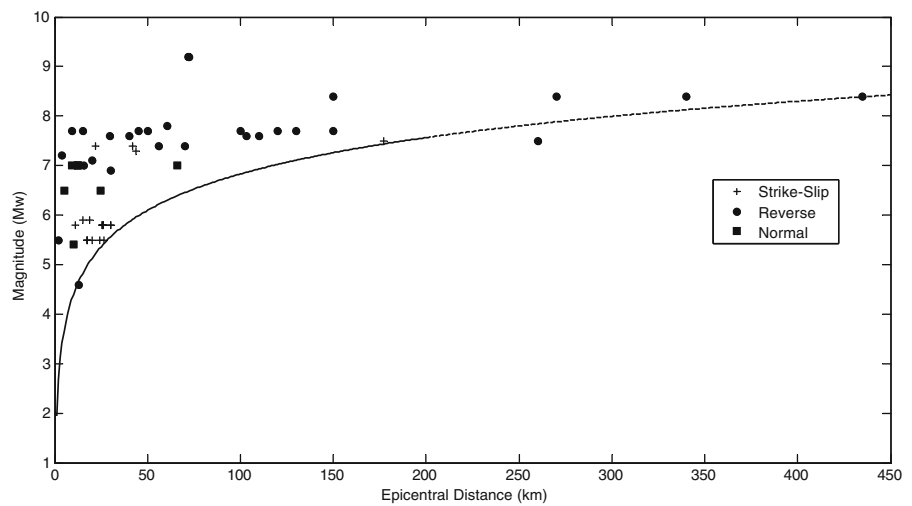
and Papathanassiou et al. – jointly fill a gap in our data set in the magnitude range between 5 and 7. In addition, the proposed lower bound by Papathanassiou et al. (2005) seems to be more conservative than ours in the range of Re under a 100 km. On the contrary, our data set seems to provide some constraints on the long-range distances of sand boil occurrence (>150 km).

Finally, we feel that our data set, based on only 30 earthquakes, has worldwide representativeness for the purposes of this paper, which is the construction of the second relationship to be discussed below, because of the partial good fits with other published curves of the same sort, as shown in Fig. 4.

4 Sand-boil diameter vs epicentral distance relationship

Out of 67 entries of sand boil reports for 30 earthquakes (Table 1), 51 of them (76% of the data set) provide the actual sizes of the blows. These were used to calculate a regression curve that relates the sand boil diameter – D – with the epicentral distance —Re (Fig. 5). The faulting type is also discriminated in the subset. The higher-bound inverse relationship between D in metres and Re in kilometres is described by Eq. 2:

$$D = 238(Re - 37)^{-0.9} \tag{2}$$

Fig. 3 Frequency of earthquake magnitude sorted by type of faulting. The uneven distribution of data along the magnitude axis precludes formulating conclusive correlations between seismotectonic parameters and liquefaction occurrence. All the same, some ideas are cautiously advanced on this respect
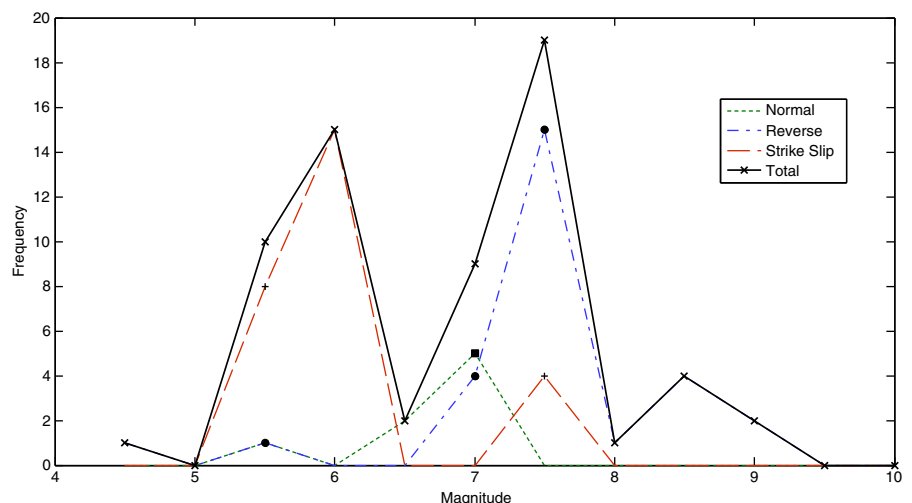
Fig. 4 Comparison of different lower-bound curves already published with the herein proposed equivalent for the magnitude vs epicentral distance relationship. Notice how curves from databases dominated by local seismotectonic conditions fit well with worldwide data with the same prevailing fault-rupture mechanism
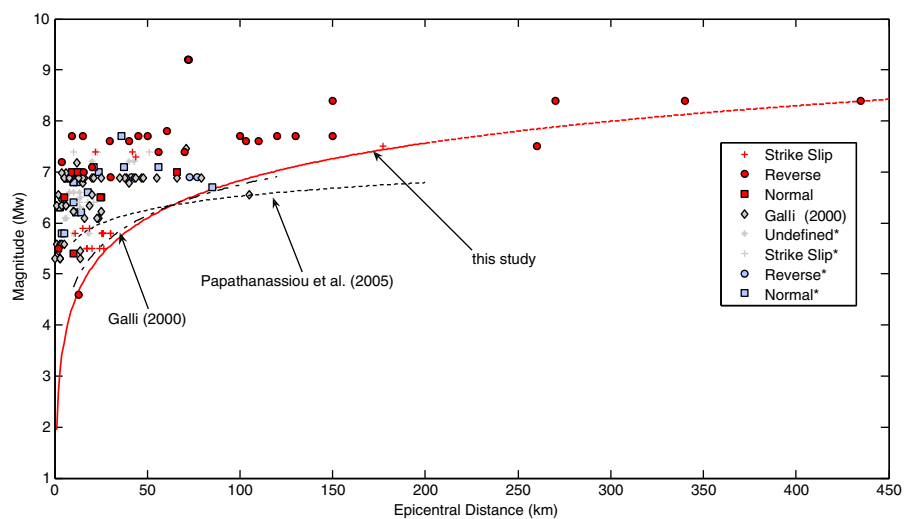
Because we are more commonly interested in deriving Re from D, Eq. 2 can be expressed as:

$$Re = (238/D)^{1.11} + 37 \qquad (3)$$

We strongly believe that this curve is not conservative at all, although large blank areas are under this upper-bound curve. We are convinced that this is due to lack of field observations that shall be filled during future earthquake investigations. We wish to express that the case described by Field et al. (1982) was intentionally left out of the regression. We believe that this sand-venting event might have been enhanced by lateral spreading. Cracks associated to mass movement increased considerably the volume of expelled sediment, making this sand boil abnormally big.

The cases plotted in Fig. 5 show that earthquakes generated by strike-slip and normal fault ruptures lead to the formation of sand blows in the near field (Re< 50 km), while those events produced during thrust faulting ruptures induce sand boils in the regional field (Re<450 km). This sand-boil size distribution is strongly dependent on the largest earthquake magnitude characteristic of each type of faulting (refer to Fig. 3).

5 Discussion

The presented empirical relationships show that source parameters seem to condition the size of sand boils. Traditionally, most of the attention has been focused on local site parameters as first-order controlling factors, and not too much has been done to define source parameter influence. Nevertheless, graphs herein presented depict how source parameters exert control on the occurrence of liquefaction to a certain extent.

Type of faulting seems to play a major role in the spatial distribution of liquefaction occurrence and size of the liquefaction features related to hydraulic fracturing. Nevertheless, an uneven distribution of magnitudes for each kind of focal solution in our database (Fig. 3) precludes clear discrimination between the controls that each one of these factors exerts on the liquefaction occurrence. However, because the larger events on Earth usually happen on thrust faults or subduction zones (Fig. 3), these events distinctively show the largest spatial distribution of sand boils (Fig. 2).
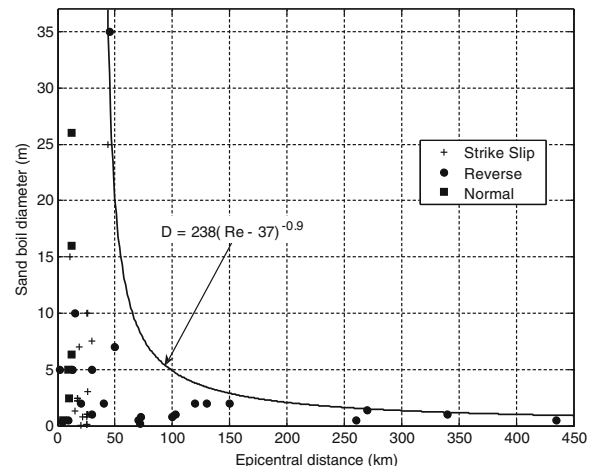

Fig. 5 Graph depicting sand boils diameter vs epicentral distance, showing an upper-bound inverse relationship

Regarding size of the hydraulically generated features, the largest ever-reported isolated sand blows occurred during the New Madrid 1811–1812 earthquake sequence, reaching diameters of up to 40 m and thickness of 0.7 m (Obermeier 1996). Although it is a historical earthquake, this value is very reliable because the sand blows are still visible in aerial photographs. This data point is not in the cross plot of Fig. 5 because no reliable epicentral distance can be determined because three large earthquakes struck the area less than 100 km apart within 3 months. Besides, the type of faulting is unknown because it was a blind-fault event that occurred in pre-instrumental time. Nevertheless, it can be postulated that these 40-m-across sand blows could be at least 20 km away from the nearest of the three epicentres, thus being satisfied by the proposed upper-bound curve (refer to Fig. 5) and corresponding Eq. 2. It is suspected, after recent investigations, that the causative fault of the 1811–1812 earthquake sequence could be an inverted high-angle normal fault. Consequently, these very large historical features could also be imputed to reverse slip. Then, it would seem that the largest ever recorded isolated sand blows are produced by thrust faulting, as a straightforward function of their very large magnitude. To illustrate this, Tuttle (2001) measured a 32-m-wide isolated sand blow, with a pool in the crater of 10×5 m, at 48 km away from the epicentre of the Gujarat 2001 Mw 7.7 earthquake, in west India.

The influence of directivity was clearly shown in the Arequipa 2001, Peru, earthquake, a 17-km-deep, Mw-8.4 seismic event with reverse rupture along a NNW–SSE fault plane, occurring within the coupled zone between the Nazca and South America plates. This event hypocentre was located near the NW end of the rupture plane. In the same way, damage, as well as induced effects, showed a completely asymmetric distribution elongated towards the SE of the focus, showing a good correlation with the aftershocks distribution and the rupture progression of the main shock (Audemard et al. 2002, 2005).

Sand boil diameter diminishes inversely with increasing epicentral distance (Fig. 5). In a similar way, wave propagation produces a change in body and surface waves amplitude at inverse rates (1/Re and 1/√Re, respectively), which indicates that wave amplitude can be an important controlling parameter in the development of these kinds of structures and their size.

We also believe that this type of study can be improved by making curves more reliable and accurate if, instead of the epicentre, the maximum energy release source is used. Nevertheless, we confidently state that the two relationships presented herein may represent a useful tool for evaluating the size of earthquakes during paleoseismic studies.

The combined use of these two curves allows determining a minimum to the actual magnitude of the investigated event, depending on the thoroughness of the sand blow mapping. The accuracy of the magnitude estimation using this method is nailed to the identification and characterisation of the farthest surveyed sand blow, which must surely lie away from the heavily damaged zone by the earthquake and must tend to be imperceptible due to its small size. Therefore, because these small sand blows are a very low to insignificant hazard, they are rarely searched for. This search necessarily relies on either the expertise of the surveyor or the accessibility to the struck region (examples of inaccessible places are deep jungle, marshes, underwater, places at war and so forth), or both. As to how these surveys are carried out, it is a fundamental issue because they should feed the existing data set in the near future. For the historical earthquakes, all depends on all aspects already discussed above, with the complementary complication that a written and/or graphical record must still exist. As to the pre-historical earthquakes, searching for the smallest and farthest sand blow is a harsh task, assuming that it was perfectly preserved in the geologic record. In such a case, the derived magnitude shall mainly be a lower bound and, very unluckily, the actual magnitude. However, a paleoseismic approach can be applied to well-documented sand blows induced by historical earthquakes, which could better constrain their magnitudes or could confirm magnitudes estimated from other approaches or data (i.e. macroseismicity studies). This would give added value to the historical seismic data. Other applications may be envisaged. For instance, using a Ms–Re curve derived from the Venezuelan catalogue that gathers records of liquefaction occurrence in association with both historical and instrumental events, Rodríguez et al. (2006) could relocate three important historical earthquakes (1530, 1797 and 1853), taking into account the Re given by the relationship.

6 Conclusions

The epicentral distance of liquefaction occurrence with respect to the magnitude of the causative earthquake can be fitted by a lower-bound curve that permits not only to estimate a radial distance within which liquefaction can be expected during future earthquakes, but also to evaluate the veracity, validity and accuracy of historical accounts, as demonstrated by Rodríguez et al. (2002, 2006) for the Venezuelan historical seismicity.

This boundary curve derived from a worldwide data set has the same shape as those from previous authors, showing a logarithmic rise of the magnitude with increasing epicentral distance. Other previous compilations, such as those of Kuribayashi and Tatsuoka (1975), Ambraseys (1991), Papadopoulos and Lefkopoulos (1993), Galli (2000) and Papathanassiou et al. (2005), were not merged with ours during this study because we pursued different aims. Our compilation intends to relate size of sand blows with characteristics of the causative earthquake, whereas the other curves only focused on the liquefaction distribution, regardless of the feature characteristics. Differences with those previously published curves are interpreted here as a result of the influence of the seismotectonics on more local databases. Particularly, the focal mechanism solution exerts a control in the behaviour of the boundary curve through the different forms of energy propagation associated with the fault type. Regardless of these slight differences, we can confidently state that the general matching of this curve with other previous relationships of the same kind validate its data set representativeness, despite having much fewer data points than those above-mentioned curves. This fact gave us confidence to propose a second curve, plotting sand-blow diameter against epicentral distance.

Still from this curve, we can determine that thrust or reverse fault earthquakes tend to produce liquefaction farther than the other two fault rupture types. For this reason, the boundary curve fitting these data is a good approximation for worldwide databases like the one gathered here. Databases of local coverage were more efficient to fit the other two kinds of fault ruptures. Nevertheless, this can be also accomplished by discriminating a worldwide database by rupture type (normal, thrust or strike-slip).

Directivity in the energy radiation away from the focus is maybe the most likely parameter controlling the above-mentioned differences, particularly in low- and medium-magnitude earthquakes. Stronger events need more data to better define the controlling factors.

The second curve, linking sand boil diameter and epicentral distance, defines an upper-bound limit that follows an inverse relationship. Seismotectonic controls on this parameter (sand boil diameter) were not clearly established, but a zoning can be determined. Thrust faulting earthquakes produce these structures in the local and regional field, while the other two styles of rupture are limited to the local field.

Used together with additional information, this kind of empirical relationship can be useful in paleoseismic surveys relying on liquefaction features as earthquake indicators. Widespread liquefaction features associated to the same given earthquake can be used to define source zones that, complemented with neotectonic data, can lead to the definition of the most likely epicentral area or causative fault. On the contrary, if the source zone is already known, its earthquake magnitude can then be derived from the magnitude vs epicentral distance curve by identifying its farthest liquefaction feature.

Sand blows can also be used to find a most likely epicentral zone when the biggest structures, associated to a given earthquake, are recognised. This epicentre should be valued in the same way as a macroseismic epicentre determination. Through using both curves and neotectonic information, the location and size of the earthquake that induced such large structures can be estimated. Historical seismicity research can also be greatly enhanced by using these empirical relationships. However, caution is recommended in the application of these relationships. Discriminated usage of them and awareness of the intrinsic limitations of these curves are key issues.

References

Alfaro P, Moretti M, Soria J (1997) Soft-sediment deformation structures induced by earthquakes (seismites) in Pliocene lacustrine deposits (Guadix-Baza Basin, Central Betic Cordillera). Eclogae Geol Helv 90:531–540

Ambraseys NN (1991) Engineering seismology. Int J Earthq Eng Struct Dyn 17:1–105

Ambraseys NN, Despeyroux J (1978) Le Tremblement de terre du 4 mars (1977) République Socialiste de Roumanie. Etude des risques naturels d'origine géophysique et des moyens d'en atténuer les effets, UNESCO, 47 p.

Atkinson GM, Liam Finn WD, Charwood RG (1984) Simple computation of liquefaction probability for seismic hazard applications. Earthq Spectra 1(1):107–123

Audemard FA, De Santis F (1991) Survey of liquefaction structures induced by recent moderate earthquakes. Bull Int Assoc Eng Geol 44:5–16

Audemard FA, Gómez J, Quijano J (2002) Efectos Geológicos Asociados al Sismo de Arequipa del 23 de Junio del 2001, Departamento de Arequipa, Perú Meridional. In: Tavera H (ed) El terremoto de la región sur del Perú del 23 de Junio del 2001, Instituto Geofísico del Perú, CD version

Audemard FA, Gómez JC, Tavera H, Orihuela N (2005) Soil liquefaction during the Arequipa Mw 8.4 June 23 2001 earthquake, southern Peru. Eng Geol 78:237–255

Bakir S, Sucuoglu H, Yilmaz T (2002) An overview of local site effects and the associated building damage in Adapazari during the 17 August 1999 Izmit earthquake. Bull Seismol Soc Am 92(1)

Barlett SF, Youd TL (1992) Empirical analysis of horizontal ground displacement generated by liquefaction-induced lateral spreads. Technical report NCEER-92-0021, State University of New York at Buffalo, National Center for Earthquake Engineering Research

Beck C, Frédéric M, Chapron E, Van Rensbergen P, De Batist M (1996) Enhanced seismicity in the early post-glacial period: evidence from the post-Würm sediments of Lake Annecy, northwestern Alps. J Geodyn 22(1/2):155–171

Castilla R, Audemard FA (2002) Licuación de sedimentos: relaciones empíricas y su aplicación a la paleosismología. In: Proceedings of III Jornadas Venezolanas de Sismología Histórica, Caracas, Venezuela. Serie Técnica FUNVISIS No 1-2002, 4pp (in CD format)

Davenport C, Ringrose P (1987) Deformation of Scottish Quaternary sediment sequence by strong earthquake motions. In: Jones ME, Preston RMF (eds) Deformation of sediments and sedimentary rocks. Special publications, vol 29. Geological Society, London, pp 299–314

Davenport CA, Lap JM, Maurenbrecher PM, Price DG (1994) Liquefaction potential and dewatering injection structures at Herkenbosch: field investigations of the effects of the 1992 Roermond earthquake, the Netherlands. Geol Mijnb 73:365–374

Ellingwood BR (1980) An investigation of the Miyagi-ken-oki, Japan, earthquake of June 12, 1978. Special publication 592, U.S. Department of Commerce, National Bureau of Standards

Field ME, Gardner J, Jennings A, Edwards BD (1982) Earthquake-induced sediment failures on a 0.25° slope, Klamath River delta, California. Geology 10:542–546

Galli P (2000) New empirical relationships between magnitude and distance for liquefaction. Tectonophysics 324:169–187

INPRES (1977) El terremoto de San Juan del 23 de Noviembre de 1977, Informe preliminar.

Kojima H, Tokimatsu K, Abe A (1992) Liquefaction-induced damage, geological and geophysical conditions during the 1990 Luzon Earthquake. In: Proceedings of the Tenth Conference Earthquake Engineering, Balkema, Rotterdam.

Kuribayashi E, Tatsuoka F (1975) Brief review of liquefaction during earthquakes in Japan. Soil Found 15:81–92

Leeds A (1983) El-Asnam, Algeria earthquake of October 10, 1980, EERI

Lekkas E, Lozios S, Skourtsos E, Kranis H (1996) Liquefaction, ground fissures and coastline change during the Egio earthquake (15 June 1995; Central-Western Greece). Terra Nova 8:648–654

López O, Malaver A, Sauter F, Lobo W, Santana G, Uzcátegui I, Gutierrez M (1992) El terremoto de Costa Rica 22 de Abril de 1991, Informe Técnico CERESIS

Maltman A (1994) The geological deformation of sediments. Chapman and Hill, London

Mariolakos I, Eleftheriou A, Mouyiaris N (1989) Seismic geological phenomena at the Kyllini area (NW Peleponnesus, Grece) induced by the Sept. 22nd and Oct. 16th 1988 earthquakes. Bull INQUA Neotecton Comm 12:62–65

Mörner N-A (1996) Liquefaction and varve deformation as evidence of paleoseismic events and tsunamis. The autumn 10,430 BP case in Sweden. Quat Sci Rev 15:939–948

Mörner N-A (2003) Paleoseismicity of Sweden. A novel paradigm. JOFO Grafiska AB, Stockholm

Munson P, Munson C-A (1996) Paleoliquefaction evidence for recurrent strong earthquakes since 20000 years BP in the Wabash Valley area of Indiana. United States Geological Survey, Reston

Munson P, Munson C-A, Pond EC (1995) Paleoliquefaction evidence for a strong Holocene earthquake in south-central Indiana. Geology 23(4):325–328

Obermeier SF (1996) Use of liquefaction-induced features for paleoseismic analysis—an overview of how liquefaction features can be distinguished from other features and how their distribution and properties of source sediment can be used to infer the location and strength of Holocene paleo-earthquakes. Eng Geol 44:1–76

Page R-A (1976) Interim report on the Guatemalan earthquake of 4 February 1976 and the activities of the U.S. Geological Survey earthquake investigation team. USGS open-file report 76-295

Papadopoulos GA, Lefkopoulos G (1993) Magnitude–distance relations for liquefaction in soil from earthquakes. Bull Seismol Soc Am 83:925–938

Papathanassiou G, Pavlides S, Christaras B, Pitilakis K (2005) Liquefaction case histories and empirical relations of earthquake magnitude versus distance from the broader Aegean region. J Geodyn 40:257–278

Pender M, Robertson T (1987) Edgecumbe earthquake: reconnaissance report. Earthq Spectra 3(4)

Prentice C, Keefer DK, Sims JD (1992) Surface effects of the earthquakes. Earthquakes & Volcanoes 23(3):127–134

Rodríguez LM, Audemard F, Rodríguez JA (2002) Casos históricos y contemporáneos de licuación de sedimentos inducidos por sismos en Venezuela desde 1530. In: Proceedings of III Jornadas Venezolanas de Sismología Histórica, Caracas, Venezuela. Serie Técnica FUNVISIS No 1-2002, 4pp (in CD format)

Rodríguez LM, Audemard FA, Rodríguez JA (2006) Casos históricos y contemporáneos de licuación de sedimentos inducidos por sismos en Venezuela desde 1530. Revista de la Facultad de Ingeniería de la Universidad Central de Venezuela, 21(3):5–32

Rodríguez Pascua MA, Calvo JP, De Vicente G, Gómez-Gras D (2000) Soft-sediment deformation structures interpreted as seismites in lacustrine deposits of the Prebetic Zone, SE Spain, and their potential use as indicators of earthquake magnitudes during the Late Miocene. Sediment Geol 135:117–135

Rodríguez Pascua MA, De Vicente G, Calvo JP, Pérez-López R (2003) Similarities between recent seismic activity and paleoseismites during the late Miocene in the external Betic Chain (Spain): relationship by "b" value and the fractal dimension. J Struct Geol 25:749–763

Seed HB, Asce M, Idriss IM (1967) Analysis of soil liquefaction: Niigata earthquake. J Soil Mech Found Div 93:83–108

Sims JD, Garvin CD (1995) Recurrent liquefaction induced by the Loma Prieta earthquake and 1990 and 1991 aftershocks: implications for paleoseismicity studies. Bull Seismol Soc Am 85(1):51–65

Sims JD (1973) Earthquake-induced structures in sediments of sediments of Van Norman Lake, San Fernando, California. Science 182:161–163

Sims JD (1975) Determining earthquake recurrence intervals from deformational structures in young lacustrine sediments. Tectonophysics 29:153–159

Singh J, Youd TL, Rollins K (1991) Geotechnical aspects. Earthq Spectra 7(Suppl B):35–40

Sukhija B, Rao M, Reddy D, Nagabhushanam P, Hussain S, Chadha R, Gupta H (1999) Paleoliquefaction evidence and periodicity of large prehistoric earthquakes in Shillong Plateau, India. Earth Planet Sci Lett 167:269–282

Tröften P-E, Mörner N-A (1997) Varved clay chronology as a means of recording paleoseismic events in southern Sweden. J Geodyn 24(1–4):249–258

Tuttle M, Law K, Seeber L, Jacob K (1990) Liquefaction and ground failure induced by the 1988 Saguenay, Quebec, earthquake. Can Geotech J 27:580–589

Tuttle M (2001) Field report on liquefaction and ground deformation survey. http://www.ceri.memphis.edu/gujarat/tuttle.shtml

Tuttle M, Seeber L (1991) Historic and prehistoric earthquake-induced liquefaction in Newbury, Massachusetts. Geology 19:594–597

Tuttle M, Cowie P, Wolf L (1992) Liquefaction induced by modern earthquakes as a key to paleoseismicity: a case study of the 1988 Saguenay event. In: Proceedings of the 1991 International Water Reactor Safety Information Meeting, Bethesda, MD, October 1991

Waag C, Lane T (1985) The Borah Peak, Idaho earthquake of October 28, 1983—Structural control of groundwater eruptions and sediment boil formation in the Chilly Buttes area. Earthq Spectra 2(1):151–168

Walsh T, Combellick R, Black G (1995) Liquefaction features from a subduction zone earthquake: preserved examples from the 1964 Alaska earthquake. Washington State Department of Natural Resources, Olympia

Wyllie LA (ed) (1986) The Chile earthquake of March 3, 1985. Earthq Spectra 2:249–506

Wyllie LA, Filson JR (eds) (1989) Armenia earthquake reconnaissance report. Earthq Spectra 5

Yamamura K, Iwasaki T, Sasaki Y, Koga Y, Taniguchi E, Tokida K (1979) Ground failures and damages to soil structures from the Miyagi-Ken-Oki, Japan earthquake of June 12, 1978. In: Proceedings U.S. National Conference on Earthquake Engineering, Stanford University, Stanford, 22–24 August 1979

Yasuda S, Tohno I (1988) Sites of liquefaction caused by the 1983 Nihonkai-Chubu earthquake. Japanese Society of Soil Mechanics and Foundation Engineering 28(2):61–72

Yegian MK, Ghahraman VG, Nogole-Sadat MA, Daraie H (1995) Liquefaction during the 1990 Manjil, Iran, Earthquake, I: case history data. Bull Seismol Soc Am 85(1):66–82

Youd TL, Perkins DM (1987) Mapping of liquefaction severity index. J Geotech Eng 113(11):1374–1392